# Population and Size Distribution of Small Jovian Trojan Asteroids

David C. Jewitt, Chadwick A. Trujillo Institute for Astronomy, University of Hawaii, 2680 Woodlawn Drive, Honolulu, HI 96822

and

Jane X. Luu

Sterrewacht Leiden

Postbus 9513, 2300RA Leiden, The Netherlands

Received	accepted
Ttecerveu	, accepted

Submitted to AJ., accepted 2000

# **ABSTRACT**

We present a study of Jovian Trojan objects detected serendipitously during the course of a sky survey conducted at the University of Hawaii 2.2-meter telescope. We used a  $8192\times8192$  pixel charge-coupled device (CCD) mosaic to observe 20 deg<sup>2</sup> at locations spread over the L4 Lagrangian swarm and reached a limiting magnitude V=22.5 mag (50% of maximum detection efficiency). Ninety-three Jovian Trojans were detected with radii  $2 \le r \le 20$  km (assumed albedo 0.04). Their differential magnitude distribution has a slope of  $0.40\pm0.05$  corresponding to a power law size distribution index  $3.0\pm0.3$  ( $1\sigma$ ). The total number of L4 Trojans with radii  $\ge 1$  km is of order  $1.6\times10^5$  and their combined mass (dominated by the largest objects) is  $\sim10^{-4}~M_{\rm Earth}$ . The bias-corrected mean inclination is  $13.7^{\circ}\pm0.5^{\circ}$ . We also discuss the size and spatial distribution of the L4 swarm.

Subject headings: asteroids – Trojans – Lagrangian points

# 1. Introduction

The Jovian Trojans are asteroidal objects confined to two swarms in Jupiter's orbit, leading and trailing the planet by 60° of longitude (known as the L4 and L5 Trojans, respectively). The first recognized Jovian Trojan (588 Achilles), discovered in 1906 by Max Wolf, was taken as providing observational confirmation of Lagrange's prediction of stable orbits at the triangular points. Currently, 132 Jovian Trojans have been numbered while another 125 await permanent designations. These objects follow loose orbits that librate around the L4 and L5 points with periods near 150 years. Recent work has shown that Trojan orbits are destabilized by collisional ejection (for which the loss rate of bodies larger

than 1 km in diameter is estimated at  $\sim 10^{-3} \text{ yr}^{-1}$ ; Marzari et al. 1997) and, to a lesser extent, by dynamical chaos (corresponding loss rate  $\sim 6 \times 10^{-5} \text{ yr}^{-1}$ ; Levison, Shoemaker and Shoemaker 1997). The implication is that the Trojans must either be the remnants of a much more substantial initial population of trapped bodies or that these objects are continually replenished from an unidentified external source.

The origin of the Trojans is a subject of much conjecture. The principal dynamical problem concerns the nature of the dissipation needed to stabilize objects in weakly bound orbits librating about L4 and L5. Schemes under consideration include capture of near-Jupiter planetesimals by gas drag in an early phase of the solar nebula (Peale 1993), stabilization of planetesimals near the L4 and L5 points due to the rapidly increasing mass of Jupiter in the late stages of its growth (Marzari and Scholl 1998), and collisional dissipation followed by capture of asteroidal fragments (Shoemaker et al. 1989). Physical observations provide only limited clues about the source of the Trojans. The optical (Jewitt and Luu 1990; Fitzsimmons et al. 1994) and near-infrared (Luu, Jewitt and Cloutis 1994; Dumas, Owen and Barruci 1998) reflection spectra appear featureless, and are reminiscent of the spectra of the nuclei of short-period comets. Like cometary nuclei, the Trojans have very low ( $\sim$ 4%) visual albedos (Cruikshank 1977; Tedesco 1989) that suggest carbonized surface compositions. If the Trojans formed near or beyond Jupiter's orbit, temperatures were probably low enough for water to exist as solid ice (rather than vapor, as in the inner nebula). This fact has led to the suggestion that the Trojans might possess ice-rich interiors equivalent to those of the cometary nuclei, a possibility which is not contradicted by any available observations (Jewitt 1996).

In this paper, we discuss the results of an optical survey taken in the direction of the L4 Jovian swarm. The survey differs from most previous work on these objects in two main respects. First, it is based on the use of a digital (CCD) detector instead of photographic

plates and so has relatively high sensitivity to faint (small) Jovian Trojans. Second, the parameters of the survey are extremely well known as a consequence of the relative ease with which digital data may be calibrated (compared to non-linear, analog photographic data). Therefore, we are able to measure the statistical properties of the L4 Trojans with greater confidence than would be possible with photographic data. A preliminary abstract describing this work (Chen et al. 1997) is superceded by the present report.

#### 2. Observations and Data Reduction

The present observations were taken as part of a study of the Kuiper Belt, the main results of which are already published (Jewitt, Luu and Trujillo 1998). Here we present observations taken UT 1996 Oct. 7 to 15 at the f/10 Cassegrain focus of the University of Hawaii 2.2-meter telescope with a  $8192\times8192$  pixel CCD mosaic (hereafter called 8k). The 8k consists of eight  $2048\times4096$  pixel Loral chips with 15  $\mu$ m pixels and gaps between chips of  $\sim$ 1 mm. The pixels were binned  $3\times3$  in order to reduce the readout time (from approximately 6 minutes to 1 minute) while maintaining Nyquist sampling of the images. The binned image scale was  $0.405\pm0.002$  "/pixel yielding a field of view  $18.4^{\circ}\times18.4^{\circ}$  (0.094 deg<sup>2</sup>). Typical image quality (including contributions from the intrinsic seeing, wind shake and tracking oscillations during the unguided integrations) varied from  $0.8^{\circ}$  to  $1.0^{\circ}$  Full Width at Half Maximum (FWHM), meaning that the images were Nyquist sampled. The images were taken with a 150-sec integration time through a specially optimized VR filter (bandwidth 5000 Å to 7000 Å; Jewitt, Luu and Trujillo 1998). Each sky position was imaged at three epochs, with a separation between epochs of about 1 hour. In total, we observed 20 deg<sup>2</sup> of sky in the direction of L4.

The data were flattened using a median combination of dithered images of the evening twilight sky. Observations of photometric standard stars (Landolt 1992) were used to

calibrate the sensitivity of each chip. By defining an A0 star to have  $m_{VR} = V = R = 0$ , an object of solar color (V - R = 0.35) has  $V \approx m_{VR} + 0.2$ . We adopted the latter relation to transform our VR magnitude to standard V magnitude in this work. Note that Trojan asteroids display a wide range of optical colors, from nearly solar to very red  $(V - R \sim 0.6)$ : Jewitt and Luu 1990, Fitzsimmons et al. 1994), leading to the introduction of small, color-dependent corrections to the V vs.  $m_{VR}$  relation. In addition, some of the 8k CCDs were of locally inferior photometric quality. Together, these effects introduce an inherent uncertainty in the absolute photometric accuracy of about 0.2 mag. Trojans were identified using the MODS detection program (Trujillo and Jewitt 1998). We determined the detection efficiency of MODS by searching for artificial objects added to real data. The efficiency is adequately fitted by the function

$$e = e_{\text{max}} \left[ 1 - \frac{1}{2} \exp\left(\frac{m_V - m_V(50)}{\sigma_V}\right) \right] \tag{1}$$

where  $e_{\rm max}$  is the maximum detection efficiency,  $m_V$  is the Trojan magnitude,  $m_V(50)$  is the magnitude at which the detection efficiency equals  $e_{\rm max}/2$ , and  $\sigma_V$  measures the width of the band of decreasing detection efficiency. When including the trailing loss due to the motion of the Trojans during the integration, we found  $e_{\rm max} = 0.86 \pm 0.01$ ,  $m_V(50) = 22.47 \pm 0.05$  and  $\sigma_V = 1.13 \pm 0.01$ . Variations in the seeing within the data are small and affect  $m_V(50)$  by at most  $\sim 0.1$  mag. (i.e., less than the formal uncertainty in the absolute photometry).

We took all observations near opposition, where the rate of retrograde motion across the sky,  $\omega$  ["/hr], is inversely related to the heliocentric distance. With this constraint we could not observe the L4 point directly, but instead mapped areas at a range of angular distances from the Lagrangian point (Figure 1). In addition, because we could not afford to interfere with our primary (Kuiper Belt) observational program, we secured no follow-up astrometry of Trojan candidates with which to determine orbital elements. Instead, we used

the sky-plane angular speed to distinguish Trojans from main-belt asteroids. The main-belt asteroids move westward at rates generally higher than the more distant Trojans, permitting us to separate the two types of object on the basis of speed. Figure 2a shows the apparent velocities in RA and Dec of numbered main-belt asteroids and previously known Trojans in the direction of our observations on 1996 October 10. The curves in Figure 2a show the loci of points having total angular motions  $\omega=22''/{\rm hr}$  and  $\omega=24''/{\rm hr}$ . At  $\omega>24''/{\rm hr}$ we find exclusively main-belt asteroids (Fig. 2a). Roughly equal numbers of main-belt and Trojan asteroids appear in the range  $22 \le \omega \le 24''/hr$ . On the other hand, a large majority (~90%) of the objects with  $\omega \leq 22''/{\rm hr}$  are Trojans. Therefore,  $\omega \leq 22''/{\rm hr}$  constitutes our operational definition of Trojans in this survey. This definition is clearly not perfect, but it is sufficiently robust that we can make statistical identifications of the Jovian Trojans in our data. Figure 2b shows all 93 Trojan candidates flagged by the detection software. Of these, only the 4th object in Table 1 has position and motion consistent with a previously known Trojan asteroid (6020 P-L). The best evidence that we have indeed obtained a sample dominated by Trojans, as opposed to foreground main-belt asteroids, is provided by the sky-plane surface density distribution of the 93 identified objects (Figure 3). This distribution is peaked towards L4 in a manner incompatible with the azimuthally uniform distribution of the main-belt asteroids.

#### 3. Discussion

# (a) Luminosity Function

Photometry was performed using a circular aperture 4.7" in projected diameter, with sky subtraction from a contiguous annulus 3" wide (Table 1). This aperture was selected by trial and error to give a stable measure of the flux while minimizing photometric noise from the background sky. The statistical photometric uncertainty is  $\pm 0.2$  mag at

the faint end and less than  $\pm 0.1$  mag at the bright end of the magnitude distribution. For comparison with other work, it is useful to employ the absolute V magnitude,  $V(1,1,0) = V - 5\log_{10}(R\Delta)$ , where R [AU] and  $\Delta$  [AU] are the heliocentric and geocentric distances, respectively. The correction to zero phase angle has been ignored (since the phase angles near opposition are small). The distances R and  $\Delta$  are not accurately known for the individual Trojan asteroids. We adopt the mean distances of the numbered L4 Trojans at the epoch of observation, namely  $R = 5.1 \pm 0.2$  AU and  $\Delta = 4.1 \pm 0.2$  AU. Here, the quoted errors are  $1\sigma$  standard deviations and the dispersion in R and  $\Delta$  results from the finite extent of the L4 swarm along the line of sight. With these values we obtain  $V(1,1,0) = V - (6.60 \pm 0.24)$ . For reference, we further compute the Trojan radii, r [km], from the relation

$$r = \sqrt{\frac{2.24 \times 10^{16 + 0.4(V_{\text{Sun}} - V(1,1,0))}}{p_V}}$$
 (2)

where  $p_V$  is the geometric albedo at the V wavelength and  $V_{\rm Sun} = -26.74$  is the apparent V magnitude of the sun. The mean geometric albedo of the Trojans recorded by the IRAS satellite (Tedesco 1989) is  $p_V = 0.040 \pm 0.005$  (however, the quoted statistical uncertainty is probably smaller than inherent systematic uncertainties due to assumptions made in the radiometric modelling of the IRAS data). With this  $p_V$ , we obtain

$$r_{0.04}[\text{km}] = 10^{0.2(24.23-V)}$$
 (3)

(Figure 4). A Trojan at the 50% detection threshhold V = 22.5 has V(1, 1, 0) = 15.9 and  $r_{0.04} = 2.2$  km. The brightest (faintest) Trojan detected in the present survey has V = 17.7(23.4) corresponding approximately to  $r_{0.04} = 20.2$  km (1.5 km). The distance variation across the diameter of the L4 swarm introduces an uncertainty to the derived radii of about  $\pm 10\%$ .

Figure 5 shows the cumulative luminosity function (CLF) computed from the present data. The "×" marks in the figure show the distribution of the raw counts while the filled circles show the distribution corrected for the detection efficiency. We have not included a correction for contamination of the Trojan sample by main-belt interlopers. As noted above, this is a small effect whose inclusion would decrease the estimated surface densities at all magnitudes by about 10%. Error bars in Figure 5 were estimated from Poisson statistics. The luminosity function is taken to be of the form

$$N(V)dV = 10^{\alpha(V-V_0)} dV \tag{4}$$

A least-squares fit to the differential magnitude distribution gives slope parameter  $\alpha = 0.40 \pm 0.05$ . The three lines in Figure 5 have gradients  $\alpha - 1\sigma$ ,  $\alpha$ , and  $\alpha + 1\sigma$ , where  $1\sigma = 0.05$ . We assume that the radii of Trojans follow a differential power law distribution such that the number of objects having radii in the range  $r \to r + \mathrm{d}r$  is  $n(r) \, \mathrm{d}r = \Gamma \, r^{-q} \mathrm{d}r$ , where  $\Gamma$  and q are constants. For objects all located at a single heliocentric and geocentric distance,  $\alpha$  and q are related by  $q = 5\alpha + 1$  (Irwin et al. 1995). Thus, the present data suggest  $q = 3.0 \pm 0.3$  in the radius range  $2.2 \le r_{0.04} \le 20$  km. For comparison, Shoemaker et al. 1989 estimated  $\alpha = 0.433$  for  $10.25 \le B(1,0) \le 14$  mag (corresponding to q = 3.17 in the approximate range  $4 \le r_{0.04} \le 40$  km, assuming  $B - V \sim 0.65$ ), but did not state their uncertainty. We consider these determinations to be in good agreement.

The difference between q measured here and the canonical q=3.5 distribution produced by collisional shattering (Dohnanyi 1969) is statistically insignificant. In any case, unmodeled effects will cause the Trojan distribution to differ from a Dohnanyi power law. For example, the velocity of ejection of collision fragments varies inversely with fragment size (as  $r^{-1/2}$ , Nakamura and Fujiwara 1991). Following collisional production the small Trojans should preferentially escape from the L4 region, leading to a distribution flatter

than the Dohnanyi power law (i.e., q < 3.5). We consider it likely that the small Trojan asteroids are collisionally produced fragments of once larger bodies (c.f. Marzari et al. 1997).

# (b) Inclination-Frequency Distribution

We are able to measure the position angles of the proper-motion vectors of the Trojans with an uncertainty of about  $\pm 1^{\circ}$ . The proper-motion vectors cannot be accurately converted to orbital inclinations without a fuller knowledge of the orbits than we possess. The approximate relation between the direction of apparent motion and the true inclination is given by

$$\tan \theta_a = \frac{\tan(i)}{\sqrt{R[1 + \tan^2(i)]} - 1} \tag{5}$$

where  $\theta_a$  is the angle between the apparent direction of motion and the projected ecliptic, i is the true orbital inclination, and R is the semi-major axis of the orbit. In deriving Eq. (5) we have assumed that the orbital eccentricities are zero, that the proper motion is the vector difference of the intrinsic motion of the Trojans from the orbital motion of earth and that the observations are taken at opposition. In the limit  $i \to 90^{\circ}$ ,  $\tan \theta_a \to R^{-1/2}$  so that with R = 5.2 AU we find  $\theta_a \to 24^{\circ}$ . One object in Table 1 has  $\theta_a > 24^{\circ}$  (#26). Presumably, it is a main belt asteroid whose sky-plane velocity falls fortuitously within the Trojan domain.

The distribution of intrinsic inclinations (Figure 6a) has a mean  $i = 7.4^{\circ} \pm 0.7^{\circ}$ , median  $i = 6.2^{\circ}$ . Trojans with large inclinations spend most of their time away from the ecliptic, leading to a bias against their detection. The bias correction varies approximately in inverse proportion to the orbital inclination. Figure 6b shows the inclination distribution after correction by the factor 1/i and normalization to Figure 6a in the range  $12 \le i \le 14^{\circ}$ . The

bias-corrected mean inclination is  $\bar{i} = 13.7^{\circ} \pm 0.5^{\circ}$  which compares favorably with Shoemaker et al.'s 1989 best estimate for the mean inclination of the larger Trojans ( $\bar{i} = 17.7^{\circ}$ ).

Observers of Trojan asteroids two decades ago suspected that "there is a possibility that the inclinations are bimodal... with groups separated by a minimum at  $i \sim 13^{\circ}$ " (Degewij and van Houten 1979). There is indeed an apparent lack of Trojans in the corrected inclination distribution with  $i = 14^{\circ} \pm 1^{\circ}$ , giving a bimodal appearance (Fig. 6b). However, inspection of the raw data in Figure 6a shows that the local minimum is statistically insignificant. Furthermore, the inclination distribution of numbered and un-numbered L4 Trojans (from an electronic list maintained by Brian Marsden at the Minor Planet Center) shows no evidence for bimodality (Figure 7). Therefore, we conclude that the data provide no compelling evidence for a bimodal distribution of inclinations.

# (c) Size and Content of the L4 Trojan Swarm

Figure 3 shows the variation of the surface density,  $\Sigma(\theta)$  [deg<sup>-2</sup>], of L4 Trojans with angular distance,  $\theta$ , from the L4 point along the ecliptic. The data can be fitted by a Gaussian function

$$\Sigma(\theta)d\theta = \Sigma_0 + \Sigma_1 \exp\left[\frac{-\theta^2}{2\sigma_T^2}\right]d\theta, \qquad (15^\circ \le \theta \le 60^\circ)$$
 (6)

with  $\Sigma_0 = 1.1 \pm 0.4$  [deg<sup>-2</sup>],  $\Sigma_1 = 27.7 \pm 4.6$  [deg<sup>-2</sup>] and  $\sigma_T = 11.2^{\circ} \pm 0.9^{\circ}$  [deg<sup>-2</sup>]. The apparent FWHM of the L4 swarm measured along the ecliptic is  $26.4^{\circ} \pm 2.1^{\circ}$ , with measurable surface density for  $\theta \leq 40^{\circ}$ . The linear size corresponding to FWHM =  $26.4^{\circ}$  is  $\sim 2.4$  AU. For comparison, Holman and Wisdom (1992) found that the theoretical stable zones of the Jupiter Lagrange point have an angular radius of about 35°. The angular half width of the swarm along the ecliptic (13.2°  $\pm$  1.0°) is comparable to the bias-corrected mean inclination (13.7°  $\pm$  0.5°), meaning that we may take the projected outline of the

swarm as approximately circular in the plane of the sky.

The number of L4 Trojans within angle  $\theta_{\text{max}}$  of L4 is then

$$N(\theta_{\text{max}}) = \int_{0^{\circ}}^{\theta_{\text{max}}} 2\pi \sin(\theta) \Sigma(\theta) d\theta.$$
 (7)

We plot solutions to Eq. (7) in Figure 8. The amplitude of libration about L4 ranges up to 60° (Shoemaker et al. 1989). Accordingly, we obtain the nominal population estimate  $N(60^{\circ}) = 3.4 \times 10^4$  ( $V \le 22.5, r_{0.04} \ge 2.2$  km), plotted in Figure 8 as Model A. The uncertainty on this number may be estimated in two ways. Uniformly increasing (decreasing) the fitted parameters  $\Sigma_0$ ,  $\Sigma_1$  and  $\sigma_T$  by  $1\sigma$  changes N by  $\pm 35\%$  (c.f. Figure 8). Systematic errors may also affect  $N(\theta_{\rm max})$ , particularly since the surface density at  $\theta \le 15^{\circ}$  is not measured in our survey. However, we find these errors to be small. If, to consider an extreme case, we arbitrarily (and unphysically) assume that  $\Sigma(\theta \le 15^{\circ}) = 0$ , we obtain (from Eq. 7)  $N(60^{\circ}) = 2.1 \times 10^4$ , still only 40% less than the nominal estimate. We conclude that  $N(\theta_{\rm max})$  is uncertain to within a factor of order 2.

The cumulative luminosity function is replotted in Figure 9, including 132 numbered and 125 unnumbered Trojan asteroids (hollow circles) from orbital element catalogs maintained by the Minor Planet Center. We used V(1,1,0) = H + 0.36 to correct the catalog magnitudes to the V band magnitudes employed here. In making the comparison between the number of Trojans deduced from the present survey (Eq. 8) with those from the Minor Planet lists, we have corrected the former by a factor of two, to account for the unobserved L5 swarm. (Early suspicions that L4 might be more populated than L5 have not been borne out by recent data, supporting our application of a factor of two, Shoemaker et al. 1989). Curvature of the CLF at  $V(1,1,0) \ge 9.5$  ( $r_{0.04} \le 42$  km) indicates observational incompleteness in the Minor Planet Trojan sample, as does the fact that the catalog asteroids are less numerous than those of the present survey by 1 to 2 orders of

magnitude in the common  $11 \le V(1,1,0) \le 14$  mag range (Figure 9). Thirty seven objects have V(1,1,0) < 9.5. Their effective CLF has slope  $\alpha = 0.89 \pm 0.15$ , significantly steeper than measured from the fainter objects of the 8k survey. The implied size distribution index is  $q = 5.5 \pm 0.9$  ( $V(1,1,0) < 9.5, r_{0.04} \ge 42$  km).

The data of Figure 9 are adequately fitted by the following differential size distributions:

$$n_1(r_{0.04}) dr_{0.04} = 1.5 \times 10^6 \left(\frac{1 \text{ km}}{r_{0.04}}\right)^{3.0 \pm 0.3} dr_{0.04} \qquad (2.2 \le r_{0.04} \le 20 \text{ km})$$
 (8)

and

$$n_2(r_{0.04}) dr_{0.04} = 3.5 \times 10^9 \left(\frac{1 \text{ km}}{r_{0.04}}\right)^{5.5 \pm 0.9} dr_{0.04} \qquad (r_{0.04} \ge 42 \text{ km}).$$
 (9)

The corresponding integral distributions are

$$N(>r_{0.04}) = 1.6 \times 10^5 \left(\frac{1 \text{ km}}{r_{0.04}}\right)^{2.0 \pm 0.3} \qquad (2.2 \le r_{0.04} \le 20 \text{ km})$$
 (10)

and

$$N(>r_{0.04}) = 7.8 \times 10^8 \left(\frac{1 \text{ km}}{r_{0.04}}\right)^{4.5 \pm 0.9} \qquad (r_{0.04} \ge 42 \text{ km})$$
 (11)

From Eq. (10) we find the number of L4 Trojans with  $r_{0.04} \geq 5$  km is  $N \sim 6400$ , to within a factor of order 2. For comparison, there were 5700 numbered and 1100 unnumbered main-belt asteroids with  $r_{0.04} \geq 5$  km as of 1999 July 29. These estimates validate the assertion by Shoemaker et al. (1989) to the effect that the populations of the main-belt and the Trojan swarms are of the same order. The number of L4 Trojans with  $r_{0.04} \geq 1$  km is  $\sim 1.6 \times 10^5$ , from Eq. (11).

The most straightforward explanation of the slope differences (Eq. 8 and 9 and Figure 9) is that the large objects represent a primordial population while Trojans smaller than a critical radius,  $r_c$ , are produced from the larger ones by collisional shattering (Shoemaker et al. 1989, Marzari et al. 1996). By equating Eqs. (10) and (11) we find  $r_c \sim 30$  km (corresponding to  $V(1,1,0)=10.2\pm0.5$  (Figure 9)). Binzel and Sauter (1992) reported that Trojans with  $r_{0.04}>45$  km have a larger mean lightcurve amplitude (a measure of elongated body shape) than their low albedo main-belt counterparts. They suggested that this might mark the primordial/fragment transition size, with larger bodies retaining the aspherical forms in which they were created (we note that this explanation is clearly non-unique). Inspection of their Figure 21 shows that the transition radius defined in this way is uncertain to within a factor of 2 and fully compatible with  $r_c \sim 30$  km as found here. We conclude that two independently measured physical parameters (the size distribution and the lightcurve amplitude distribution) show evidence for a change near  $r_c \approx 30$  km to 40 km.

The total mass of Trojans is

$$M_T = \int_0^{r_c} \frac{4}{3} \pi \rho n_1(r) dr + \int_{r_c}^{\infty} \frac{4}{3} \pi \rho n_2(r) dr$$
 (12)

where  $n_1$  and  $n_2$  are from Eqs. (8) and (9) and  $\rho = 2000 \text{ kg m}^{-3}$  is the assumed bulk density. We find  $M_T \approx 5 \times 10^{20} \text{ kg} \approx 9 \times 10^{-5} M_{\text{Earth}}$ , equivalent to a 400 km radius sphere having the same density. Dynamical calculations show that escaped Trojans would be quickly scattered into orbits indistinguishable from those of some short-period comets (Marzari et al. 1995). Therefore it is of interest to compare  $M_T$  with the mass of short-period comets delivered to the inner solar system over the past 4.5 Gyr. The rate of supply of short period comets is  $f \sim 10^{-2} \text{ yr}^{-1}$  (Fernandez 1985). The size and mass distributions of the cometary nuclei have not been adequately measured. We assume that the nuclei

follow a differential size distribution with index q=3 and minimum and maximum radii  $r_1=0.5$  and  $r_2=30$  km. The mass-weighted mean radius drawn from this distribution is  $\bar{r}\approx (2r_2r_1^2)^{1/3}=2.5$  km. A small number of well-measured cometary nuclei have radii  $\sim$  few km (Jewitt 1996), consistent with this estimate. The delivered mass of short-period comets is then  $M_C\approx 4\pi\rho\bar{r}^3fT/3$ , where  $T=4.5\times 10^9$  yr is the age of the solar system. We find  $M_C\approx 6\times 10^{21}$  kg, corresponding to  $M_C\approx 10~M_T$ . This mass, if taken at face value, makes it unlikely that the Trojan swarms could be the dominant source of the comets. It is entirely possible, however, that a fraction of the short-period comets could be escaped Trojans. A definitive estimate of this fraction will require better knowledge of the cometary parameters  $(r_1, r_2, q, f,$  and density) than we now possess, as well as detailed understanding of the physics of collisional ejection from the Trojan swarms.

The present results were extracted from data taken for an independent (Kuiper Belt) purpose. They serve to give an idea of the power of modern CCD arrays on a telescope of rather modest diameter. Much more could be learned from a survey specifically targeting the Trojan asteroids and including astrometric follow-up, so that orbital elements can be determined for individual objects. Future work should focus on a more complete digital survey of both L4 and L5 swarms in order to determine the total population and size distribution with greater confidence. Observations taken away from the ecliptic will provide a better measure of the high inclination objects. Observations to fainter limiting magnitudes will allow us to probe the sub-kilometer population. Carefully planned observations will produce stronger constraints on the collisional and dynamical states of the Jovian Trojans, leading ultimately to a deeper understanding of these enigmatic bodies.

# 4. Summary

- The luminosity function of the Jovian L4 Trojans has slope of 0.40 ± 0.05 in the magnitude range 18.0 ≤ V ≤ 22.5, corresponding to objects with radii 2 ≤ r<sub>0.04</sub> ≤ 20 km (where r<sub>0.04</sub> is the radius derived assuming a geometric albedo of 0.04). The corresponding differential power law size distribution index is q = 3.0±0.3. This is consistent with the slope expected for a collisionally shattered population (q ~ 3.5; Dohnanyi 1969) within ~ 2σ (95%) confidence and suggests that the small Trojans are collisional fragments of larger bodies.
- 2. The brighter (larger) Trojans follow a  $q = 5.5 \pm 0.9$  differential power law distribution.
- 3. The apparent FWHM of the L4 swarm is  $26^{\circ} \pm 2^{\circ}$ , measured along the ecliptic.
- 4. The distribution of inclinations of the Trojans, when corrected for observational bias, has a mean  $13.7^{\circ} \pm 0.5^{\circ}$ .
- 5. About  $1.6 \times 10^5$  L4 Trojans are bigger than 1 km radius. Their combined mass is of order  $5 \times 10^{20}$  kg  $(9 \times 10^{-5} M_{\rm Earth})$ , assuming bulk density  $\rho = 2000$  kg m<sup>-3</sup>.

# Acknowledgements

We thank John Dvorak for operation of the UH telescope. Gerry Luppino, Mark Metzger, Richard Wainscoat and Pui Hin Rhoads helped us with the camera and the computer set-up. We benefitted from digital lists of Trojan orbital elements maintained by Brian Marsden and David Tholen. Scott Sheppard and an anonymous referee provided helpful comments. This research was supported by grants from NASA to DCJ.

#### REFERENCES

Binzel, R. P. and Sauter, L. M. 1992. Icarus 95, pp. 222-238.

Chen, J., Jewitt, D., Trujillo, C., and Luu, J. 1997. Bull. Am. Astr. Soc 29, 25.08.

Cruikshank, D. 1977. Icarus 30, 224-230.

Degewij, J., and van Houten, C. J. 1979. In *Asteroids*, ed. T. Gehrels (Univisity of Arizona Press, Tucson), pp. 417-435.

Dohnanyi, J. 1969. J. Geophys. Res. **74**, pp. 2531-2554.

Dumas, C., Owen, T., and Barucci, M. 1998. Icarus 133, 221-232.

Fernandez, J. A. 1985. Icarus 64, pp. 308-319.

Fitzsimmons, A., Dahlgren, M., Lagerkvist, C.-I., Magnusson, P., and Williams, I.P. 1994.

Astron. Ap. 282, 634-642

Holman, M., and Wisdom, J. 1993. A. J. 105, pp.1987-1999.

Irwin, M., Tremaine, S., and Zytkow, A. 1995. A. J. 110, 3082.

Jewitt, D. C. and Luu, J. X. 1990. A. J. **100**, 933-944.

Jewitt, D. 1996. Earth, Moon and Planets **72**, 185-201.

Jewitt, D., Luu, J. and Trujillo, C. 1998. A. J. 115, 2125-2135.

Landolt, A. 1992. A. J. **104**, 340 - 371.

Levison, H. F., Shoemaker, E. M. and Shoemaker, C. S. 1997. Nature 385, pp.42-44.

Marzari, F., Farinella, P., and Vanzani, V. 1995. Astron. Ap. 299, 267-276.

Marzari, F., Scholl, H., and Farinella, P. 1996. Icarus **119**, pp. 192-201.

Marzari, F., Farinella, P., Davis, D. R., Scholl, H. and Bagatin, A. C. 1997. Icarus 125, pp. 39-49.

Marzari, F., and Scholl, H. 1998. Astron. Ap. 339, 278-285.

Nakamura, A., and Fujiwara, A. 1991. Icarus **92**, 132-146.

Peale, S. 1993. Icarus 106, 308.

Shoemaker, E. M., Shoemaker, C. S. and Wolfe, R. F. 1989. In *Asteroids II*, eds. Binzel, R.P., Gehrels, T. and Matthews, M. S. (University of Arizona Press, Tucson), pp. 487-523.

Tedesco, E. F. 1989. In *Asteroids II*, eds. Binzel, R.P., Gehrels, T. and Matthews, M. S. (University of Arizona Press, Tucson), pp. 1090-1138.

Trujillo, C. and Jewitt, D. 1998. A. J. 115, 1680-1687.

This manuscript was prepared with the AAS  $\LaTeX$  macros v5.0.

# FIGURE CAPTIONS

- **Figure 1**. The sky coverage of the present survey is marked by squares. The L4 Lagrangian point is marked by a large filled circle and the ecliptic is shown for reference.
- Figure 2. (a) Apparent angular velocities of numbered main-belt asteroids (empty circles) and Trojans (filled circles) projected in the direction of observation on 1996 October 10. Marked curves show angular velocities  $\omega = 22''/\text{hr}$  and 24''/hr. (b) Objects detected by MODS having  $\omega \leq 24''/\text{hr}$ : those with  $\omega \leq 22''/\text{hr}$  are taken to be Trojans for the purpose of this study. All objects moving faster than  $\omega = 24''/\text{hr}$  are main-belt asteroids and were ignored by the MODS software.
- Figure 3. Surface density variation of the observed L4 swarm along the ecliptic. A Gaussian distribution with  $\sigma_T = 11.2 \pm 0.9$  (corresponding to FWHM is  $26.4^{\circ} \pm 2.1^{\circ}$ ) fits the data.
- Figure 4. Magnitude vs. size relation for Trojan asteroids (Eq. 2).
- Figure 5. Cumulative magnitude-frequency distribution of detected Trojans. Crosses mark the original data; filled circles indicate the distribution after correction for the detection efficiency. The straight lines have gradients  $\alpha = 0.35$ , 0.40 and 0.45.
- Figure 6. (a) Apparent distribution of inclinations of Trojans found in the present survey. (b) Same as (a) but corrected for inclination bias and normalized at  $12^{\circ} \le i \le 14^{\circ}$ .
- Figure 7. Inclination distribution of the L4 Trojans (numbered + unnumbered).
- Figure 8. Cumulative number of Trojans with radii  $\geq 2.2$  km (the smallest objects detected in the present survey) as a function of angular distance from the L4 point. Model A shows Eq. (7) with  $\Sigma_0 = 1.1 \pm 0.4$ ,  $\Sigma_1 = 27.7 \pm 4.6$  and  $\sigma_T = 11.2 \pm 0.9$  in the range  $0^{\circ} \leq \theta \leq 60^{\circ}$ . Model B is the same as Model A except that  $\Sigma_0 = \Sigma_1 \equiv 0$  for  $\theta \leq 15^{\circ}$ .

Uncertainties on both curves show the effect of forcing  $\Sigma_0$ ,  $\Sigma_1$  and  $\sigma_T$  to  $+1\sigma$  and  $-1\sigma$  from the best-fit values.

**Figure 9**. Cumulative luminosity function from this work (filled circles) and from 257 cataloged Trojans detected in earlier surveys (empty circles). Counts from the present survey have been doubled to account for the unobserved L5 swarm.

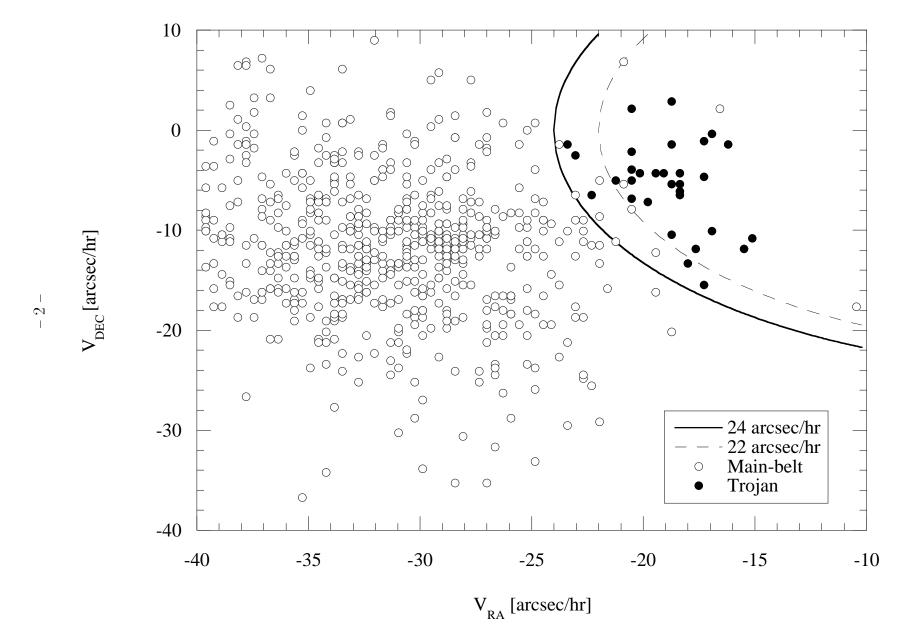
Table 1. Trojan Asteroids from the 8k Survey

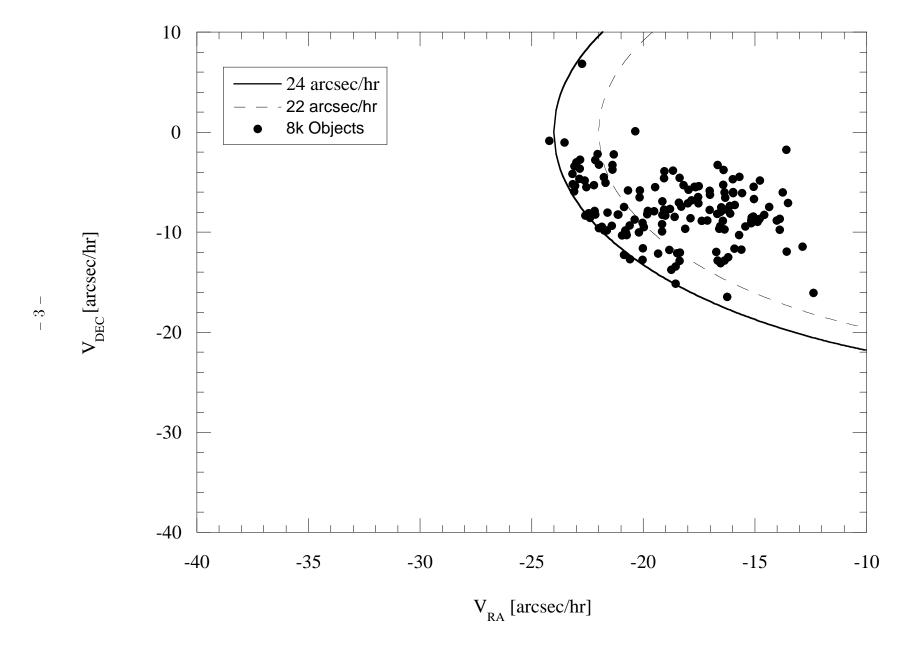
<u> </u>						
V	D [km]	$i [\deg]$	N	V	D [km]	$i [\deg]$
17.7	40.9	22.8	48	21.6	6.7	1.5
17.8	40.1	2.2	49	21.6	6.8	1.8
18.7	26.4	9.6	50	21.7	6.4	10.8
18.8	25.2	2.1	51	21.8	6.2	0.6
18.9	23.5	12.1	52	21.8	6.1	3.8
19.0	22.8	5.4	53	21.8	6.2	4.5
19.5	18.2	0.3	54	21.8	6.4	0.7
19.7	16.0	6.5	55	21.8	6.3	8.3
19.7	16.1	6.2	56	21.9	6.1	3.2
19.8	15.8	8.7	57	21.9	5.9	5.6
19.8	15.8	6.7	58	21.9	6.0	5.4
20.0	14.2	7.7	59	21.9	6.0	1.6
20.1	13.9	15.9	60	21.9	5.9	3.7
20.1	13.7	5.0	61	21.9	5.9	5.2
20.4	11.7	20.0	62	21.9	5.9	20.7
20.5	11.3	16.1	63	22.0	5.7	0.8
20.6	10.8	8.3	64	22.0	5.7	2.6
20.6	10.9	8.5	65	22.0	5.7	16.7
20.6	10.6	9.1	66	22.1	5.4	7.4
20.7	10.2	7.2	67	22.2	5.1	7.6
20.7	10.4	0.4	68	22.2	5.2	7.9
20.8	9.6	1.7	69	22.2	5.3	17.7
20.8	9.9	8.0	70	22.2	5.2	4.1
20.8	10.0	7.6	71	22.3	5.1	5.7
20.8	9.9	0.3	72	22.3	4.9	6.2
	17.7 17.8 18.7 18.8 18.9 19.0 19.5 19.7 19.8 20.0 20.1 20.1 20.4 20.5 20.6 20.6 20.6 20.7 20.7 20.8 20.8	17.7       40.9         17.8       40.1         18.7       26.4         18.8       25.2         18.9       23.5         19.0       22.8         19.5       18.2         19.7       16.0         19.7       16.1         19.8       15.8         19.8       15.8         20.0       14.2         20.1       13.9         20.1       13.7         20.4       11.7         20.5       11.3         20.6       10.8         20.6       10.9         20.6       10.6         20.7       10.4         20.8       9.6         20.8       9.9         20.8       10.0	17.7       40.9       22.8         17.8       40.1       2.2         18.7       26.4       9.6         18.8       25.2       2.1         18.9       23.5       12.1         19.0       22.8       5.4         19.5       18.2       0.3         19.7       16.0       6.5         19.7       16.1       6.2         19.8       15.8       8.7         19.8       15.8       6.7         20.0       14.2       7.7         20.1       13.9       15.9         20.1       13.7       5.0         20.4       11.7       20.0         20.5       11.3       16.1         20.6       10.8       8.3         20.6       10.8       8.3         20.6       10.6       9.1         20.7       10.2       7.2         20.7       10.4       0.4         20.8       9.6       1.7         20.8       9.9       8.0         20.8       10.0       7.6	17.7       40.9       22.8       48         17.8       40.1       2.2       49         18.7       26.4       9.6       50         18.8       25.2       2.1       51         18.9       23.5       12.1       52         19.0       22.8       5.4       53         19.5       18.2       0.3       54         19.7       16.0       6.5       55         19.7       16.1       6.2       56         19.8       15.8       8.7       57         19.8       15.8       6.7       58         20.0       14.2       7.7       59         20.1       13.9       15.9       60         20.1       13.7       5.0       61         20.4       11.7       20.0       62         20.5       11.3       16.1       63         20.6       10.8       8.3       64         20.6       10.9       8.5       65         20.6       10.6       9.1       66         20.7       10.4       0.4       68         20.8       9.6       1.7       69	17.7       40.9       22.8       48       21.6         17.8       40.1       2.2       49       21.6         18.7       26.4       9.6       50       21.7         18.8       25.2       2.1       51       21.8         18.9       23.5       12.1       52       21.8         19.0       22.8       5.4       53       21.8         19.5       18.2       0.3       54       21.8         19.7       16.0       6.5       55       21.8         19.7       16.1       6.2       56       21.9         19.8       15.8       8.7       57       21.9         19.8       15.8       6.7       58       21.9         20.0       14.2       7.7       59       21.9         20.1       13.9       15.9       60       21.9         20.1       13.7       5.0       61       21.9         20.4       11.7       20.0       62       21.9         20.5       11.3       16.1       63       22.0         20.6       10.8       8.3       64       22.0         20.6       10.9 <t< td=""><td>17.7       40.9       22.8       48       21.6       6.7         17.8       40.1       2.2       49       21.6       6.8         18.7       26.4       9.6       50       21.7       6.4         18.8       25.2       2.1       51       21.8       6.2         18.9       23.5       12.1       52       21.8       6.1         19.0       22.8       5.4       53       21.8       6.2         19.5       18.2       0.3       54       21.8       6.4         19.7       16.0       6.5       55       21.8       6.3         19.7       16.1       6.2       56       21.9       6.1         19.8       15.8       8.7       57       21.9       5.9         19.8       15.8       6.7       58       21.9       6.0         20.0       14.2       7.7       59       21.9       6.0         20.1       13.9       15.9       60       21.9       5.9         20.1       13.7       5.0       61       21.9       5.9         20.4       11.7       20.0       62       21.9       5.9      &lt;</td></t<>	17.7       40.9       22.8       48       21.6       6.7         17.8       40.1       2.2       49       21.6       6.8         18.7       26.4       9.6       50       21.7       6.4         18.8       25.2       2.1       51       21.8       6.2         18.9       23.5       12.1       52       21.8       6.1         19.0       22.8       5.4       53       21.8       6.2         19.5       18.2       0.3       54       21.8       6.4         19.7       16.0       6.5       55       21.8       6.3         19.7       16.1       6.2       56       21.9       6.1         19.8       15.8       8.7       57       21.9       5.9         19.8       15.8       6.7       58       21.9       6.0         20.0       14.2       7.7       59       21.9       6.0         20.1       13.9       15.9       60       21.9       5.9         20.1       13.7       5.0       61       21.9       5.9         20.4       11.7       20.0       62       21.9       5.9      <

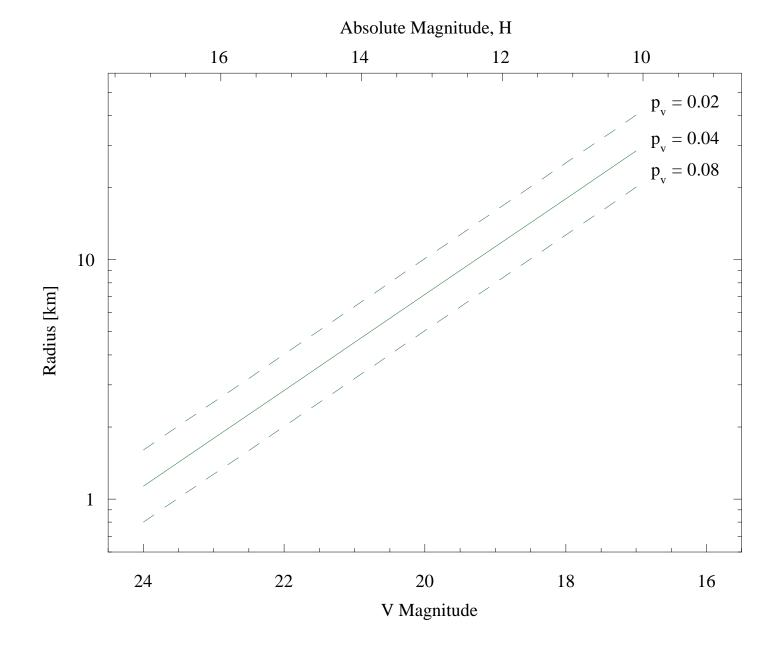
Table 1—Continued

$\overline{N}$	V	D [km]	$i [\deg]$	N	V	D [km]	$i [\deg]$
			. 01				
26	20.9	9.2	29.2	73	22.3	4.9	4.8
27	20.9	9.6	12.8	74	22.3	4.8	25.7
28	20.9	9.3	8.7	75	22.4	4.7	20.0
29	20.9	9.3	9.3	76	22.4	4.7	7.3
30	21.0	8.9	5.7	77	22.4	4.7	2.4
31	21.0	9.0	1.8	78	22.4	4.7	1.0
32	21.1	8.7	2.2	79	22.5	4.5	6.4
33	21.1	8.6	8.9	80	22.6	4.3	0.6
34	21.1	8.6	18.8	81	22.6	4.4	3.5
35	21.1	8.7	8.0	82	22.6	4.4	11.9
36	21.1	8.6	7.2	83	22.7	4.2	2.4
37	21.3	7.7	3.7	84	22.7	4.1	1.2
38	21.3	7.8	3.4	85	22.8	4.0	0.5
39	21.4	7.4	6.0	86	22.8	4.0	2.0
40	21.5	7.1	10.7	87	22.9	3.7	2.4
41	21.5	7.2	1.2	88	22.9	3.8	19.4
42	21.5	7.3	10.2	89	23.0	3.5	3.8
43	21.5	7.1	3.6	90	23.1	3.4	9.5
44	21.5	7.2	8.8	91	23.2	3.3	0.1
45	21.6	7.0	2.1	92	23.3	3.1	1.9
46	21.6	7.0	16.5	93	23.4	2.9	21.5
47	21.6	6.8	6.2				

Right Ascension [deg]







-5-

